Exploring the relationship between a fluid container's geometry and when it will balance on edge

Ryan J. Moriarty
California Polytechnic State University

Contents

Introduction

At some point while consuming a beverage, many people will idly try to balance its container on edge. The act itself is physically straightforward, merely involving the system's center of mass and achieving a static equilibrium between the opposing torques caused by gravity and the normal force between the container and the surface on which it balances. Further analysis of the act, however, illuminates the richness of the exercise.

These nuances are apparent even in simplified two-dimensional models because of the depth of the relationship between a container's geometry and achieving balance. The purpose of such analysis is threefold: first, when considering a rectangular container, to determine the relationship between the angle at which it balances and the amount of fluid in the container; second, to consider a massless analogue to a standard twelve-ounce aluminum can which balances at a fixed angle and observe the interplay between the various parameters of that container's geometry and balance; and finally, to revisit the aluminum can model, this time considering its mass relative to the fluid's, and recover the familiar behavior observed when balancing real-world beverages in aluminum cans.

1 Rectangular container

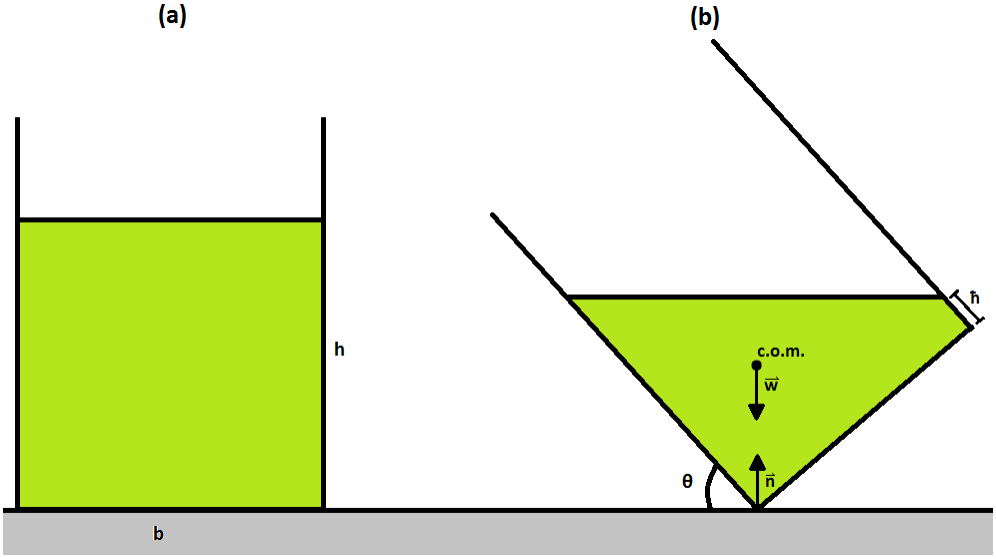

Figure 1: Two-dimensional rectangular container filled to height h with liquid resting on its base, width b, (left), and balancing on its edge (right).

To facilitate this analysis, the fluid in the container will be treated as uniformly dense. As such, calculating the center of mass simply requires calculating the centroid of a given fluid shape. There are two regimes for the geometry of the fluid while its container is balanced on edge. The first to consider, which exhibits the richest behavior, is seen in Fig. (1). Later, the second regime where the fluid height in the tilted frame sits at or below the elevated corner, will be explored.

It is worth nothing that Fig. (1) also illustrates the definition of balance. Its center of mass, labeled *c.o.m.*, rests directly above the corner of the container in contact with the surface. By definition, for the container to be balanced, i.e., in mechanical equilibrium, the net force and net torque on the system must both be zero. Per Newton's Third Law, the normal force and the weight of the fluid are equal in magnitude but antiparallel, satisfying the first condition for mechanical equilibrium. Because the container rests at an angle θ such that there is no perpendicular distance between either force vector and the corner of the container in contact with the surface about which it could pivot, the net torque is zero, satisfying the second and final condition for mechanical equilibrium.

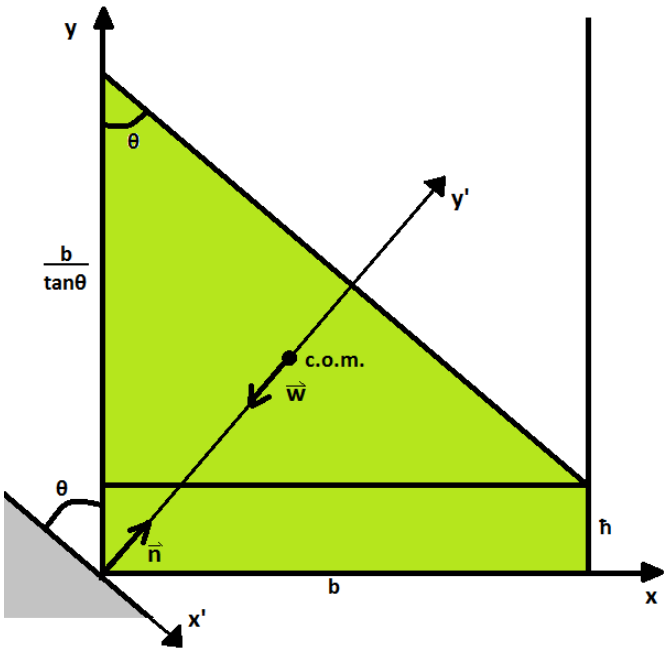

Figure 2: Rectangular container balanced on edge in the first geometric regime.

1.1 The first geometric regime

The variable $\hbar$ is significant to the analysis of the rectangular container in this regime, but its algebraic relationship with the other known parameters isn't immediately apparent. Setting the area of the fluid, bh, equal to the sum of the areas of the two shapes in Fig. (2), i.e., $bh = b\hbar + \frac{b^2}{2\tan\theta}$, it follows that, for a given untilted fluid height h and balancing angle θ,

$$\hbar = h - \frac{b}{2\tan\theta}. \tag{1}$$

By taking a weighted average of the centroids of the triangle and rectangle which constitute the fluid shape seen in Fig. (2), the x and y coordinates of the tilted fluid's center of mass are

$$(\bar{x}, \bar{y}) = \frac{1}{bh}\left[b\hbar\left(\frac{b}{2}, \frac{\hbar}{2}\right) + \frac{b^2}{2\tan\theta}\left(\frac{b}{3}, \hbar + \frac{b}{3\tan\theta}\right)\right]. \tag{2}$$

After substituting Eq. (1) into Eq. (2), $\bar{x}$ and $\bar{y}$ become

$$\bar{x} = \frac{b}{2} - \frac{b^2}{12h\tan\theta}, \tag{3}$$

and

$$\bar{y} = \frac{h}{2} + \frac{b^2}{24h\tan^2\theta}. \tag{4}$$

As noted before, when the system is in static equilibrium, the center of mass is directly above the corner on which the container balances. When such balance is achieved the x'-coordinate of the fluid's center of mass on the rotated axis shown in Fig. (2) will be zero, meaning that

$$\bar{x}' = \bar{x}\sin\theta - \bar{y}\cos\theta = 0 \tag{5}$$

must be satisfied.

Substituting Eqs. (3) and (4) into Eq. (5), then multiplying through by $\frac{h}{b^2}$, it follows that the quadratic

$$\left(\frac{h}{b}\right)^2 - \tan\theta\left(\frac{h}{b}\right) + \frac{1}{6}\left(\frac{1}{2\tan^2\theta} + 1\right) = 0 \tag{6}$$

must also be satisfied for the container to achieve balance.

From the well-known quadratic formula and Eq. (6), $\left(\frac{h}{b}\right)$ as a function of θ in this regime is

$$\left(\frac{h}{b}\right) = \frac{\tan\theta}{2} + \sqrt{\frac{\tan^2\theta}{4} - \frac{1}{6}\left(\frac{1}{2\tan^2\theta} + 1\right)}. \tag{7}$$

While it would be preferable to have found the inverse relationship, such a relationship cannot be found due to the transcendental nature of Eq. (7).

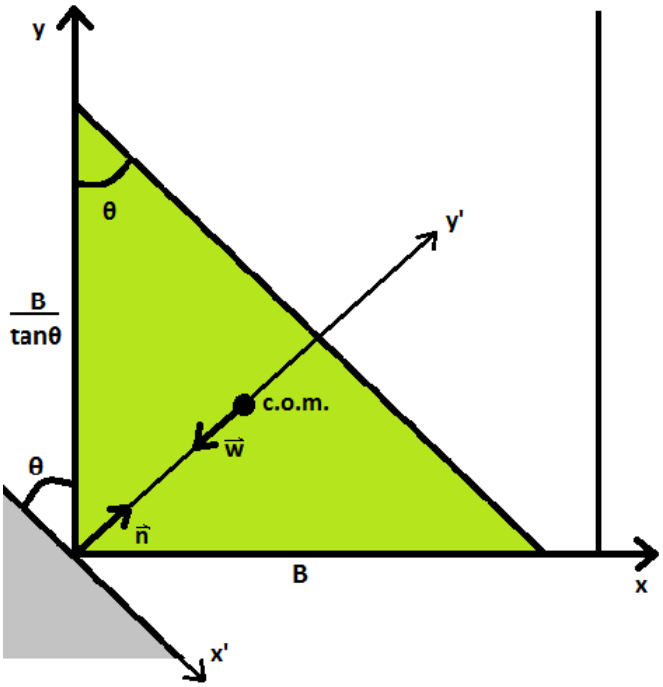

Figure 3: Rectangular container balanced on edge when $\left(\frac{h}{b}\right) \leq \frac{1}{2}$.

1.2 The second geometric regime

It is important to recall that Eq. (7) is only true in the geometric regime of Figs. (1) and (2). That is, it only holds true so long as the tilted fluid height sits above the far corner of the container. Restated in more concrete, algebraic terms, it is true only while $\left(\frac{h}{b}\right) \geq \frac{1}{2}$, which will be apparent later.

In the second geometric regime, shown in Fig. (3), the variable, B, has been introduced to facilitate this analysis. The center-of-mass calculation is more straightforward in the second regime, as the fluid is simply in the shape of a triangle with the centroid located at

$$(\bar{x}, \bar{y}) = \frac{1}{bh}\left[\frac{B^2}{2\tan\theta}\left(\frac{B}{3}, \frac{B}{3\tan\theta}\right)\right]. \tag{8}$$

Applying the rotational transform of Eq. (5) and recalling that the x'-coordinate of the center of mass must once again fall at the origin, the condition required for balance to be achieved in this regime is

$$\frac{B}{3\tan\theta} = \frac{B}{3}\tan\theta. \tag{9}$$

There is only one angle, $\theta = \frac{\pi}{4}$, for which Eq. (9) holds true. Thus, the intuitive result

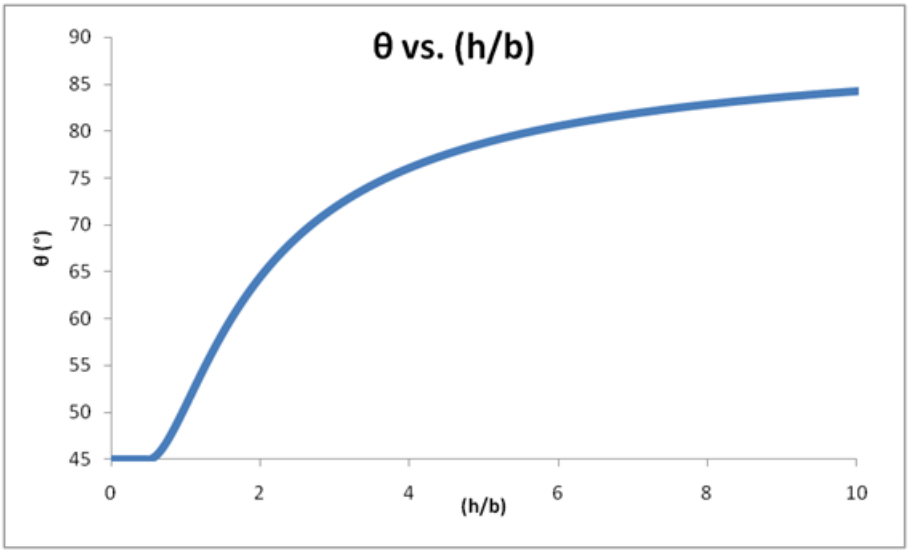

Figure 4: Graph of θ against $\left(\frac{h}{b}\right)$.

for achieving balance in this regime has been recovered: the geometry of Fig. (3) yields a right triangle with equal-length catheti.

Between Eqs. (7) and (9), the massless rectangular container has been solved in each of the possible geometric regimes.

In Fig. (4), the complete behavior of the massless rectangular container is illustrated. In the limit where $\left(\frac{h}{b}\right) \to \infty$, (that is, when $h >> b$) the balancing angle θ approaches $\frac{\pi}{2}$. On the other extreme, when $\left(\frac{h}{b}\right) \leq \frac{1}{2}$, the balancing angle θ remains at $\frac{\pi}{4}$.

2 The single-slotted container

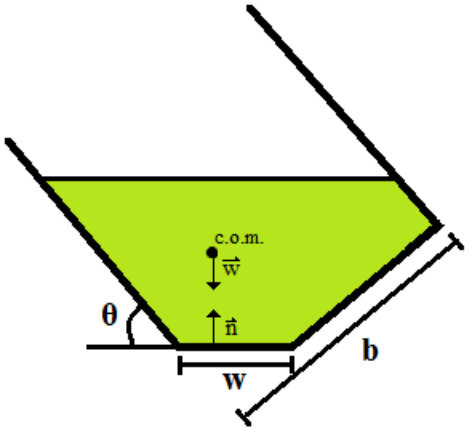

Figure 5: The single-slotted container balanced on its slotted edge

In solving the rectangular container, one uncovers relationship between the properties of it and the fluid it contains and the angle at which it will balance. However, a common real-life experiment is to attempt to balance an aluminum can on the beveled edge which surrounds its base. In that problem, the balancing angle is instead a fixed parameter of the container's geometry and the conditions for balance are a function of that geometry.

Fig. (5) shows the two-dimensional model which will be used for analyzing the behavior observed when attempting to balance aluminum cans on their bevel. For balance, i.e. mechanical equilibrium, to be achieved in this model, the system's center of mass must be directly above the container's slot. If the center of mass is to the left of the slot, gravitational torque will tip the container anticlockwise onto its side. Similarly, if the center of mass is to the right of the slot, the torque will tip it clockwise back onto its base.

For the rectangular container filled with fluid height h, balance is always achieved at some angle θ. However, in this model, for a container of base b, slot width w and fixed balancing angle θ containing fluid of height h, balance is only achieved when the center of mass of the system falls within the "window" of the container's slot width.

Analysis of the single-slotted container to approximate the behavior observed when balancing an aluminum can on its bevel, then, is concerned with the "trajectory" of the center of mass of the fluid in the tilted container as a function of the fluid's height when the container is upright.

2.1 Geometric regimes and meta-regimes

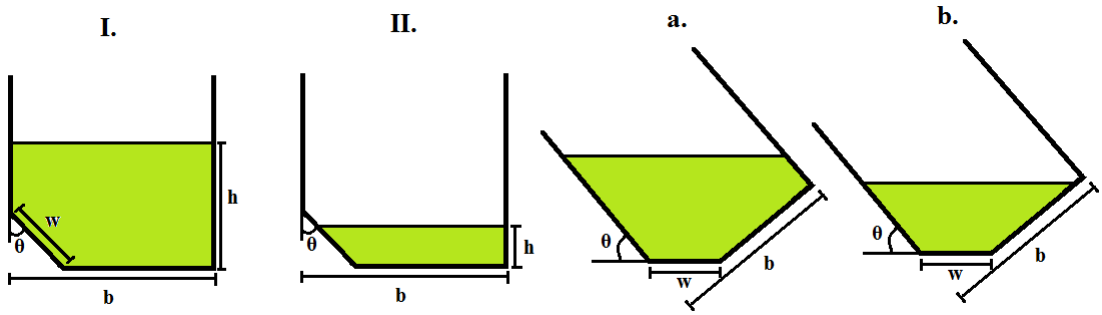

Figure 6: The four possible geometric regimes for the single-slotted container, I and II being the untilted fluid geometries, and (a) and (b) the tilted fluid geometries.

As was done with the rectangular container, the four fluid geometries shown in Fig. (6) will be delineated by expressions involving the untilted fluid height h. To do this a schematic graph of the three meta-regimes of the fluid's geometry will be utilized.

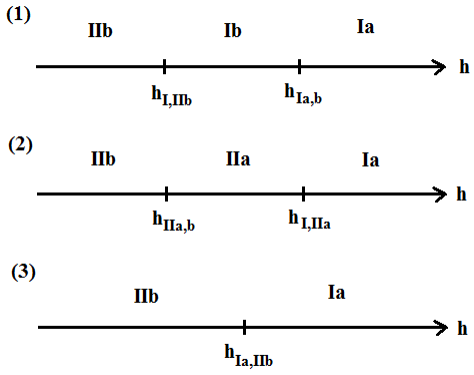

Figure 7: Schematic detailing the three geometric meta-regimes of the single-slotted container.

In Fig. (7), an Arabic numeral indicates a unique meta-regime. A roman numeral combined with a lowercase letter (e.g., IIb) indicates which tilted and untilted geometric regimes from Fig. (6) are observed in a particular container for a range of h values. For example, regime Ia corresponds to a container with fluid height h which has the untilted fluid geometry of diagram I in Fig. (6) and the tilted geometry of diagram (a) also seen in Fig. (6). An h with subscripts (e.g., $h_{I,IIb}$) indicates a crossover fluid height at which a new geometric regime - tilted, untilted or both - occurs. For example, $h_{Ia,b}$ indicates the h

value at which fluid geometry transitions from regime Ia to Ib as h is decreased, and $h_{I,IIa}$ indicates the geometric transition between regimes Ia and IIa as h decreases, and so forth.

These crossover heights are derived in Appendix A. Stated here without proof they are

$$h_{I,IIa} = h_{I,IIb} = h_{Ia,IIb} = w\cos\theta, \tag{10}$$

$$h_{Ia,b} = \frac{b}{2\tan\theta}, \tag{11}$$

and

$$h_{IIa,b} = \frac{-(b - w\sin\theta) + \sqrt{2b\,(b - w\sin\theta)}}{\tan\theta}. \tag{12}$$

With Eqs. (10), (11) and (12) the behavior of the fluid geometry as a function of h is now known within each of the three meta-regimes. However, these crossover heights do not diagram the way in which a container's geometry determines which meta-regime in which it operates.

The third meta-regime is a good starting point for this discussion, because the crossovers from I to II and from (a) to (b) from Figure (6) occur simultaneously for the same height, $h = h_{Ia,IIb}$.

Another condition for this simultaneity involves the parameter V, which is diagramed in the next section. This condition, which a container's geometry must satisfy to operate in meta-regime (3), is

$$V = 0, \tag{13}$$

where the general form of V is

$$V = \frac{1}{b\cos\theta}\left[A + \frac{1}{2}w^2\sin\theta\cos\theta\right] - \frac{b}{2\sin\theta}, \tag{14}$$

when $h = h_{Ia,IIb}$, where A is the area of the fluid in the container. As seen in Fig. (6), the fluid area can be expressed in regimes I and II, respectively, as

$$A_I = bh - \frac{1}{2}w^2\sin\theta\cos\theta. \tag{15}$$

$$A_{II} = h(b - w\sin\theta) + \frac{1}{2}h^2\tan\theta \tag{16}$$

Combining Eqs. (10), (13), (14) and (15) yields

$$b = 2w\sin\theta, \tag{17}$$

the relationship of the spacial parameters of the container which must be satisfied for it to exhibit the behavior of meta-regime (3).

In meta-regime (1), the fluid geometry transitions between tilted regimes (a) and (b) while remaining in untilted regime I. It follows, then, that when $h = h_{Ia,b}$ the untilted fluid level must be above the high corner of the slot, i.e.,

$$h_{Ia,b} > w\cos\theta. \tag{18}$$

Substituting Eq. (11) into the inequality of Eq. (18) yields

$$b > 2w\cos\theta, \tag{19}$$

the relationship of the spatial parameters of the container which defines meta-regime (1).

Containers which occupy meta-regime (2) transition between untilted regimes I and II while remaining in the tilted regime (a). By inspection of the geometry of tilted regime (a), the condition

$$V > 0 \tag{20}$$

must hold true when $h = h_{I,IIa}$. It must also be noted that for the container to maintain its geometric shape its slot cannot extend past its unslotted corner, i.e., $b > w\sin\theta$. This combined with Eqs. (10), (14) and (20) yields

$$w\sin\theta < b < 2w\sin\theta, \tag{21}$$

the relationship of the container's spatial parameters which defines meta-regime (2).

Between Eqs. (19), (21) and (17), the affect of a specific container's dimensions on the behavior its fluid geometry as a function of untilted fluid height is fully mapped out for all three meta-regimes detailed in Figure (7).

2.2 Center of mass calculations

The goal of analyzing the single-slotted container is to determine the range of untilted fluid heights for which a container of base b, slot width w and balancing angle θ will balance. Because the real-life exercise of attempting to balance an aluminum can on its bevel generally involves subtracting the fluid from an initially full can by drinking it, a good starting point for discussing the fluid's center of mass is tilted regime (a) from Fig. (7), because it describes the tilted fluid geometry of any container for a sufficiently large untilted fluid height h.

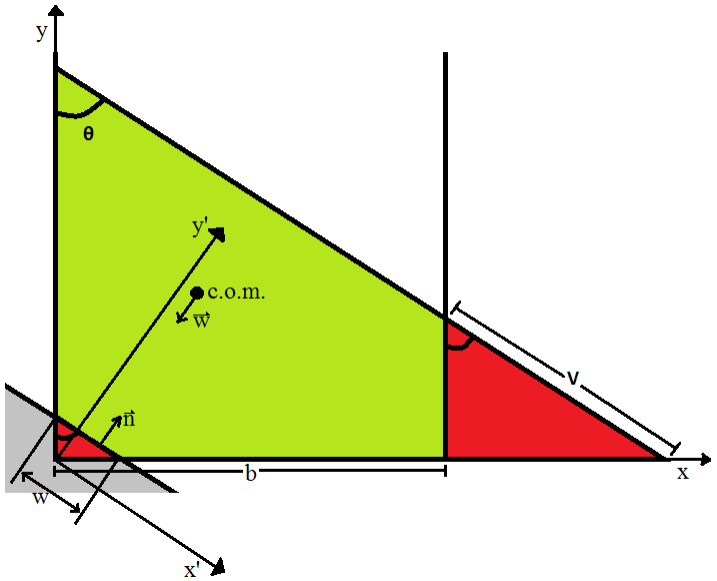

Figure 8: Labeled geometry of tilted regime (a).

Figure (8) details the geometry of tilted regime (a) for the purpose of calculating its center of mass. To accomplish this, the green-shaded fluid (area A), red-shaded triangle with hypotenuse w (area $\frac{1}{2}w^2 \sin\theta\cos\theta$), red-shaded triangle with hypotenuse V (area $\frac{1}{2}V^2 \sin\theta\cos\theta$) and the large triangle composed of the three other shapes (area $\frac{(b+V\sin\theta)^2}{2\tan\theta}$) will be considered. The centroids of these shapes can be related to each other by the expression

$$\begin{aligned}\frac{(b+V\sin\theta)^2}{2\tan\theta}\left(\frac{b+V\sin\theta}{3},\frac{b+V\sin\theta}{3\tan\theta}\right) &= A(\bar{x},\bar{y}) \\ &+ \frac{1}{2}w^2\sin\theta\cos\theta\left(\frac{w\sin\theta}{3},\frac{w\cos\theta}{3}\right) \\ &+ \frac{1}{2}V^2\sin\theta\cos\theta\left(b+\frac{V\sin\theta}{3},\frac{V\cos\theta}{3}\right), \quad (22)\end{aligned}$$

where $(\bar{x},\bar{y})$ is once again the center of mass of the tilted fluid with area

$$A_a = \frac{(b+V\sin\theta)^2}{2\tan\theta} - \frac{1}{2}w^2\sin\theta\cos\theta - \frac{1}{2}V^2\sin\theta\cos\theta \quad (23)$$

It follows from Eq. (22), then, that the center of mass of the fluid in tilted regime (a)

is

$$(\bar{x},\bar{y}) = \frac{1}{A}\left[\frac{(b+V\sin\theta)^2}{2\tan\theta}\left(\frac{b+V\sin\theta}{3},\frac{b+V\sin\theta}{3\tan\theta}\right)\right.$$
$$-\frac{1}{2}w^2\sin\theta\cos\theta\left(\frac{w\sin\theta}{3},\frac{w\cos\theta}{3}\right)$$
$$\left.-\frac{1}{2}V^2\sin\theta\cos\theta\left(b+\frac{V\sin\theta}{3},\frac{V\cos\theta}{3}\right)\right]. \quad (24)$$

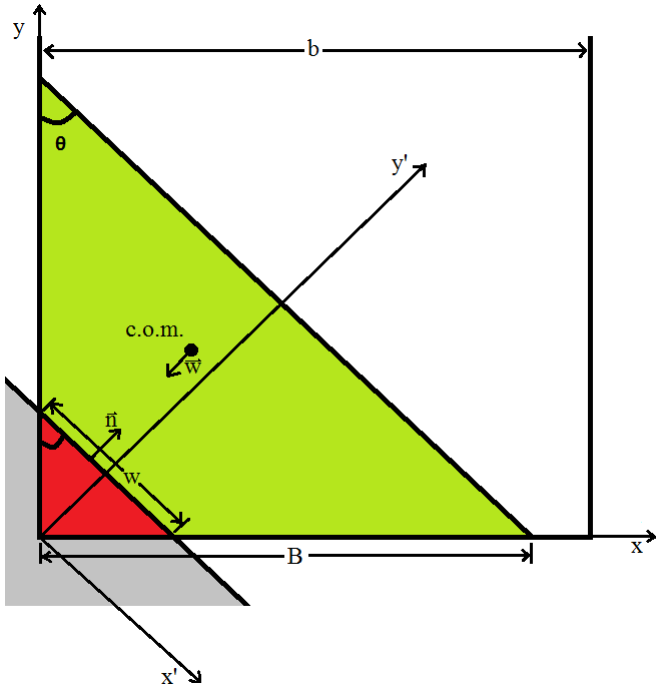

Figure 9: Labeled geometry of tilted regime (b).

Figure (9) outlines the geometry of tilted regime (b) for the purpose of determining the fluid's center of mass. To this end, the green-shaded fluid (area A), red-shaded triangle with hypotenuse w (area $\frac{1}{2}w^2\sin\theta\cos\theta$) and larger triangle with base B (area $\frac{B^2}{2\tan\theta}$) will be considered.

Because the area of the triangle with base B is equal to the sum of the other two shapes' areas, it follows that

$$B = \left[2\tan\theta\left(A+\frac{1}{2}w^2\sin\theta\cos\theta\right)\right]^{\frac{1}{2}}. \quad (25)$$

The three shapes' centroids are related by the expression

$$\frac{B^2}{2\tan\theta}\left(\frac{B}{3},\frac{B}{3\tan\theta}\right) = A(\bar{x},\bar{y}) + \frac{1}{2}w^2\sin\theta\cos\theta\left(\frac{w\sin\theta}{3},\frac{w\cos\theta}{3}\right), \tag{26}$$

from which it follows that the center of mass of the fluid in tilted regime (b) is

$$(\bar{x},\bar{y}) = \frac{1}{A}\left[\frac{B^2}{2\tan\theta}\left(\frac{B}{3},\frac{B}{3\tan\theta}\right) - \frac{1}{2}w^2\sin\theta\cos\theta\left(\frac{w\sin\theta}{3},\frac{w\cos\theta}{3}\right)\right] \tag{27}$$

and its area is

$$A_b = \frac{B^2}{2\tan\theta} - \frac{1}{2}w^2\sin\theta\cos\theta, \tag{28}$$

where B is given by Eq. (25) and A is determined by either Eq. (15) or (16), depending on its untilted geometry.

2.3 Window of balance

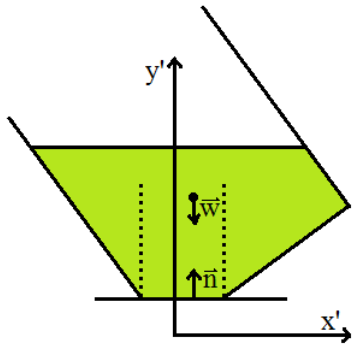

Figure 10: A detailed diagram of the single-slotted container's window of balance.

Now that the center of mass $(\bar{x},\bar{y})$ is expressed for both tilted fluid geometries, the analysis of the single-slotted container returns to the idea of balance. To be in the window of balance for this container means that the center of mass must lay above or between the edges of the slot when turned on its side. By inspection, the (x,y) coordinates for these two edges are $(0, w\cos\theta)$ and $(w\sin\theta, 0)$. Applying the rotational transform from Eq. (5) to these boundaries as well as to the coordinates of the fluid's center of mass yields

$$-w\cos^2\theta \le \bar{x}\sin\theta - \bar{y}\cos\theta \le w\sin^2\theta, \tag{29}$$

the mathematical expression of the container's window of balance.

2.4 Balancing window reentry

For any container of base b, slot width w and balancing angle $0 < \theta < \frac{\pi}{2}$, where $\left(\frac{b}{w}\right) > \sin\theta$, there is a range of untilted fluid heights for which Eq. (29) is satisfied and balance is achieved. However, one can imagine that there exist container geometries in which the fluid's center of mass eventually leaves the balance window for a range of h values, such that gravitational torque will turn the container upright, i.e.

$$\bar{x}' = \bar{x}\sin\theta - \bar{y}\cos\theta > w\sin^2\theta. \tag{30}$$

An inspection of the container's geometry reveals that for certain container geometries, as h decreases, reentry can occur in either regime (a) or (b). The center of mass, however, can only leave the balance window in regime (a), because in regime (b) the fluid's center of mass always decreases along a line interpolated between the centroids of the two triangles shown in Figure (9), $\left(\frac{1}{3}b, \frac{1}{3}\frac{b}{\tan\theta}\right)$ and $\left(\frac{1}{2}w\sin\theta, \frac{1}{2}w\cos\theta\right)$.

It follows, then, that if Eq. (30) is to be satisfied in regime (b), it must be satisfied at the crossover between regimes (a) and (b) when $V = 0$ and $B = b$. From Eq. (28), the fluid's area at the turning point is

$$A = \frac{b^2}{2\tan\theta} - \frac{1}{2}w^2\sin\theta\cos\theta. \tag{31}$$

Substituting Eqs. (31) and (27) along with the turning point condition $B = b$ into Eq. (30), then rearranging the terms such that it is a third-order polynomial function of $\left(\frac{b}{w}\right)$ yields

$$\frac{1}{3}\left(1 - \frac{1}{\tan^2\theta}\right)\left(\frac{b}{w}\right)^3 - \sin\theta\left(\frac{b}{w}\right)^2 + \frac{1}{3}\sin\theta\left(1 + \sin^2\theta\right) > 0, \tag{32}$$

the inequality which a container's geometry must satisfy for balancing window reentry to occur in regime (b).

Substituting the formula for the fluid's center of mass in regime (a) from Eq. (24) into the condition for balancing window reentry in Eq. (30) yields the quadratic inequality

$$\alpha V^2 + \beta V + \gamma > 0, \tag{33}$$

with coefficients

$$\alpha = -\frac{1}{2}\cos^2\theta b, \tag{34}$$

$$\beta = \frac{1}{2}\sin\theta\left(1 - \frac{1}{\tan^2\theta}\right)b^2 - \sin^2\theta w b, \tag{35}$$

and

$$\gamma = \frac{1}{6}\left(1 - \frac{1}{\tan^2\theta}\right)b^3 + \frac{1}{6}\sin\theta\left(1 + \sin^2\theta\right)w^3 - \frac{1}{2}\sin\theta w b^2. \tag{36}$$

The solution to the quadratic in the inequality of Eq. (33) is

$$V = \frac{-\beta \pm \sqrt{\beta^2 - 4\alpha\gamma}}{2\alpha}. \tag{37}$$

V is always positive in tilted regime (a). As a result, Eqs. (33) and (37) become

$$\frac{-\beta + \sqrt{\beta^2 - 4\alpha\gamma}}{2\alpha} > 0 \tag{38}$$

and

$$\frac{-\beta - \sqrt{\beta^2 + 4\alpha\gamma}}{2\alpha} > 0. \tag{39}$$

Eqs. (38) and (39) determine how, if at all, reentry occurs in regime (a) of a particular single-slotted container.

If both Eqs. (38) and (39) are satisfied, then the center of mass will leave and subsequently reenter the balancing window in regime (a). If only Eq. (39) is satisfied, then the inequality of Eq. (32) will also be satisfied and the center of mass will leave the balancing window in regime (a) and then reenter in regime (b). When neither Eq. (38) nor (39) is satisfied, then Eq. (32) will also not be satisfied and the container will not exhibit the phenomenon of reentry.

Because only real V values are physical and useful to this analysis, the discriminant, $\left(\beta^2 - 4\alpha\gamma\right)$, being positive determines the boundaries of the inequalities in Eqs. (38) and (39).

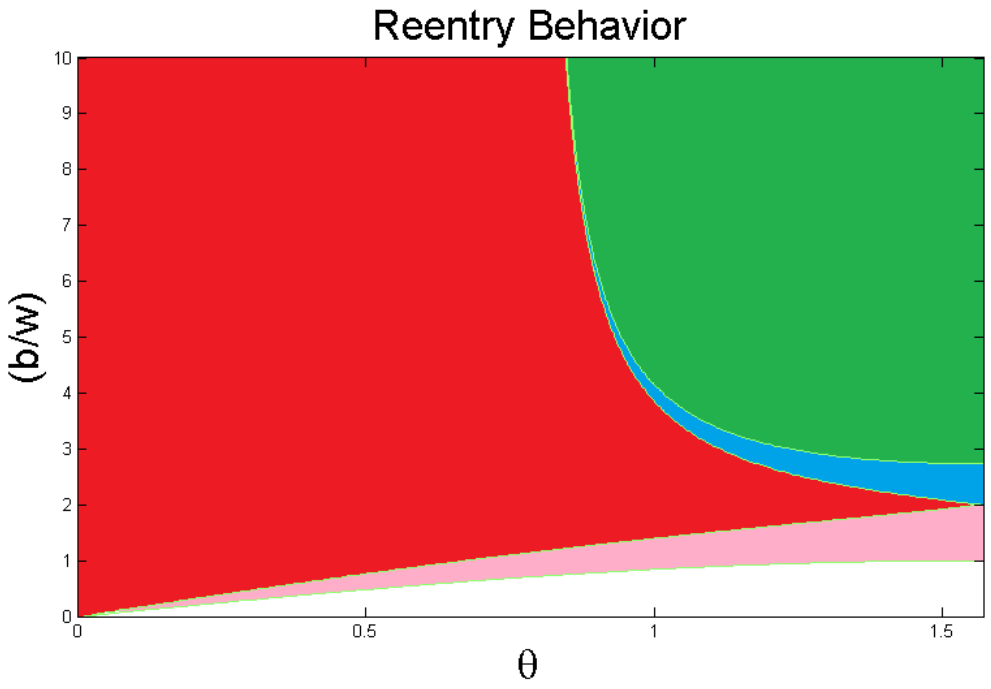

Figure 11: $\left(\frac{b}{w}\right)$ versus θ with different regimes for center-of-mass behavior highlighted.

Figure (11) is a graph of the curves resulting from setting the third-order polynomial in Eq. (32) equal to zero and from setting the discriminant from Eq. (37) equal to zero in a $\left(\frac{b}{w}\right)$-versus-θ parameter space in the ranges $0 < \left(\frac{b}{w}\right) < 10$ and $0 < \theta < \frac{\pi}{2}$. The resulting graph shows reentry behavior for all single-slotted container geometries.

The white area of the graph indicates when $b < w \sin\theta$, the region where the single-slotted container doesn't maintain its geometry so it is ignored in this analysis.

The red-shaded area indicates the range of container geometries for which Eqs. (32), (38) and (39) are not satisfied and reentry does not occur.

In the boundary between the red- and pink-shaded areas, Eq. (37)'s discriminant is zero.

In the pink-shaded region, the discriminant of Eq. (37) is positive, but Eqs. (38), (39) and (32) are not satisfied so reentry doesn't occur.

The boundary between the red- and blue-shaded areas, where the discriminant of Eq. (37) is zero, is the range of container geometries for which the center-of-mass turning point occurs in regime (a), at the edge of the balancing window, but Eqs. (32) (38) and (39) are not satisfied and reentry does not occur.

The blue-shaded area indicates the container geometries for which the center of mass leaves and subsequently reenters the balancing window in regime (a). In this region, both Eq. (38) and (39) are satisfied, but Eq. (32) is not.

The boundary between the green and blue regions, where the polynomial in Eq. (32) equals zero, indicates the geometries for which reentry occurs at the turning point between tilted regimes (a) and (b) when $B = b$ and $V = 0$.

Finally, the green-shaded region indicates containers for which the center of mass leaves the balancing window in regime (a) and then reenters the window in regime (b). In this region, Eq. (38) is not satisfied, but Eqs. (32) and (39) are.

2.5 Illustrative center of mass trajectories

So far the single-slotted container's center of mass behavior has been illustrated only in abstract terms. To observe the phenomena described by the somewhat esoteric analysis of the previous section, it is helpful to plot $(\bar{x}, \bar{y})$ for a range of untilted fluid heights h within the corresponding container geometry.

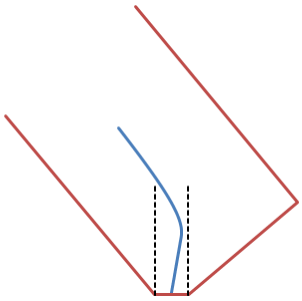

Figure 12: Center of mass trajectory for a container with $\left(\frac{b}{w}\right) = 5$ and $\theta = 50°$.

Figure (12) shows a container whose geometry does not permit the center of mass of the fluid it contains to overshoot the balancing window. As such, its geometry falls in the red area of the parameter space graph of Figure (11).

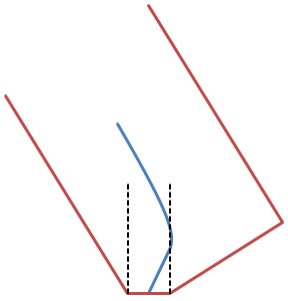

Figure 13: Center of mass trajectory for a container with $\left(\frac{b}{w}\right) = 4$ and $\theta = 58°$.

Figure (13) shows a container whose geometry is such that its fluid's center of mass overshoots and subsequently reenters the balancing window in regime (a). Consequently,

its geometry places it in the blue region of Figure (11).

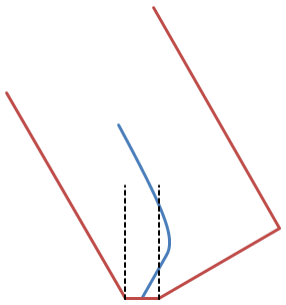

Figure 14: Center of mass trajectory for a container with $\left(\frac{b}{w}\right) = 5$ and $\theta = 60°$.

Figure (14) illustrates a container with geometric parameters such that its fluid's center of mass leaves the balancing window in regime (a) then reenters in regime (b), putting it in the green region of Figure (11).

2.6 Considering the container's mass

Because real-world twelve-ounce aluminum cans aren't massless, when attempting to balance them on their bevel one observes that for a sufficiently small amount of fluid the can will fall onto its side. This is because the x' coordinate of the can's center of mass falls short of the balancing window and its mass is sufficiently larger than the mass of the remaining fluid to bring the can-fluid system's total center of mass short of the balancing window.

To incorporate this behavior into the model of the single-slotted container, the container's mass M will be defined as

$$M = cb^2, \tag{40}$$

where c is an arbitrary, variable constant used to determine the relative mass of the container compared to fluid of area b^2.

Because aluminum cans are more or less horizontally symmetric, the container's center of mass will be located at

$$\left(\bar{X}, \bar{Y}\right) = \left(\frac{b}{2}, kb\right), \tag{41}$$

where k is a constant used to determine how far up the y-axis the container's center of mass is located.

Using the familiar analysis of the previous sections, the center of mass of the container-fluid system can be expressed as

$$\left(\bar{x}_{tot}, \bar{y}_{tot}\right) = \frac{1}{M + A}\left[A\left(\bar{x}, \bar{y}\right) + \frac{1}{M}\left(\bar{X}, \bar{Y}\right)\right], \tag{42}$$

where A and $(\bar{x}, \bar{y})$ are determined by Eqs. (23) and (24) or Eqs. (28) and (27), depending on which geometric regime applies for a given untilted fluid height h.

2.6.1 Center of mass behavior

A similar analysis to that of Section 2.4 can be utilized to determine the behavior of the container-fluid system's total center of mass for a container of base b, slot width w, balancing angle θ and coefficients c and k.

As before, to determine the center of mass trajectory in tilted fluid regime (a)'s behavior, one must look at when the x component of the system's center of mass is at the edges of the balancing window, i.e. when

$$\bar{x}'_{tot} = \bar{x}_{tot} \sin\theta - \bar{y}_{tot} \cos\theta = w \sin^2\theta \tag{43}$$

and

$$\bar{x}'_{tot} = \bar{x}_{tot} \sin\theta - \bar{y}_{tot} \cos\theta = -w \cos^2\theta. \tag{44}$$

Substituting Eq. (42) into Eq. (43) yields a quadratic of V with the form of Eq. (37) with coefficients

$$\alpha_1 = -\frac{1}{2}\cos\theta \left(\frac{b}{w}\right), \tag{45}$$

$$\beta_1 = \left(\frac{1}{2}\sin\theta - \frac{\cos\theta}{2\tan\theta}\right)\left(\frac{b}{w}\right)^2 - \sin^2\theta \left(\frac{b}{w}\right), \tag{46}$$

and

$$\gamma_1 = \left[\frac{1}{2}\sin\theta\left(c + \frac{1}{c\tan\theta}\right) - \cos\theta\left(ck + \frac{1}{6\tan^2\theta}\right)\right]\left(\frac{b}{w}\right)^3 - \sin^2\theta\left(c + \frac{1}{2\tan\theta}\right)\left(\frac{b}{w}\right)^2 + \frac{1}{6}\sin\theta\cos\theta\left(1 + \sin^2\theta\right). \tag{47}$$

Substituting Eq. (42) into Eq. (44) yields a quadratic of V with coefficients

$$\alpha_2 = -\frac{1}{2}\cos\theta \left(\frac{b}{w}\right), \tag{48}$$

$$\beta_2 = \left(\frac{1}{2}\sin\theta - \frac{\cos\theta}{2\tan\theta}\right)\left(\frac{b}{w}\right)^2 + \cos^2\theta \left(\frac{b}{w}\right), \tag{49}$$

and

$$\gamma_2 = \left[\frac{1}{2}\sin\theta\left(c + \frac{1}{3\tan\theta}\right) - \cos\theta\left(ck + \frac{1}{6\tan^2\theta}\right)\right]\left(\frac{b}{w}\right)^3 + \cos^2\theta\left(c + \frac{1}{2\tan\theta}\right)\left(\frac{b}{w}\right)^2 - \frac{1}{6}\sin\theta\cos\theta\left(1 + \cos^2\theta\right). \tag{50}$$

Once again, the sign of the discriminant determines the sign of the solution to the quadratic, so the equations which determine the system's center of mass behavior in regime (a) for a container of coefficients c and k in a $\left(\frac{b}{w}\right)$-versus-θ parameter space are

$$\beta_1^2 - 4\alpha_1\gamma_1 = 0 \tag{51}$$

and

$$\beta_2^2 - 4\alpha_2\gamma_2 = 0. \tag{52}$$

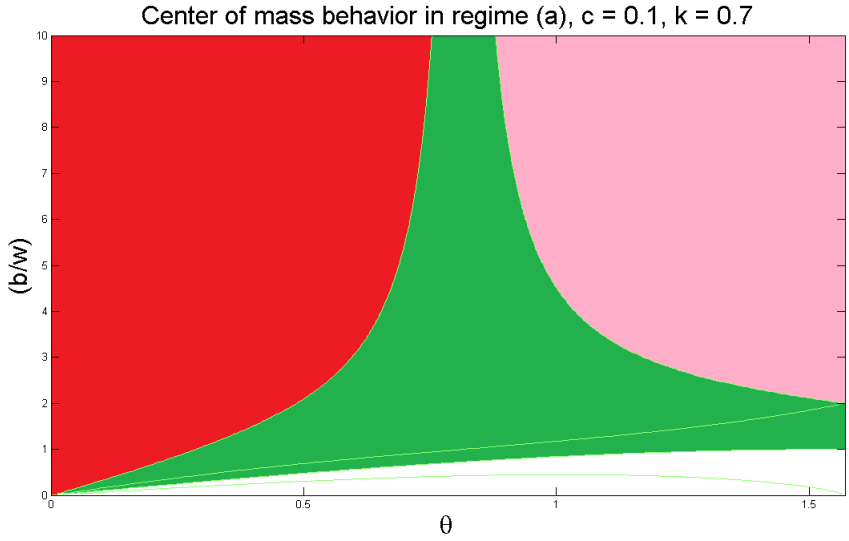

Figure 15: Parameter-space graph for a container with center of mass coefficients $c = 0.1$ and $k = 0.7$ highlighting its center of mass' behavior in tilted fluid geometry regime (a).

Figure (15) is the result of plotting Eqs. (51), (52) and $\left(\frac{b}{w}\right) = \sin\theta$ for a container with coefficients $c = 0.1$ and $k = 0.7$. The red-shaded portion of the graph indicates container geometries for which the center of mass never enters the balancing window in regime (a). The green-shaded portion indicates geometries for which the center of mass enters the window of balance in (a), but does not leave it in (a). The pink-shaded region indicates geometries for which the center of mass enters the balancing window in (a) and subsequently overshoots the window in (a). The white portion, as before, indicates the region in which $b < w\sin\theta$ where the container does not maintain its geometry and as a result isn't part of this analysis.

Figure (15), however, says nothing about the way the container's center of mass behaves in regime (b). To determine the behavior of the center of mass in regime (b), the values of B which satisfy Eqs. (43) and (44) must be analyzed. Combining Eqs. (27), (42), (43)

and (44) yield the polynomials

$$\left(\frac{1}{2}\sin\theta c - \cos\theta ck\right)\left(\frac{b}{w}\right)^3 + \left(\frac{\sin\theta}{6\tan\theta} - \frac{\cos\theta}{6\tan^2\theta}\right)\left(\frac{B}{w}\right)^3 - \sin^2\theta c\left(\frac{b}{w}\right)^2 - \frac{\sin^2\theta}{2\tan\theta}\left(\frac{B}{w}\right)^2 + \frac{1}{6}\sin\theta\cos\theta\left(1+\sin^2\theta\right) = 0 \quad (53)$$

and

$$\left(\frac{1}{2}\sin\theta c - \cos\theta ck\right)\left(\frac{b}{w}\right)^3 + \left(\frac{\sin\theta}{6\tan\theta} - \frac{\cos\theta}{6\tan^2\theta}\right)\left(\frac{B}{w}\right)^3 + \cos^2\theta c\left(\frac{b}{w}\right)^2 + \frac{\cos^2\theta}{2\tan\theta}\left(\frac{B}{w}\right)^2 - \frac{1}{6}\sin\theta\cos\theta\left(1+\cos^2\theta\right) = 0. \quad (54)$$

Because Eqs. (53) and (54) are three dimensional polynomials, the center of mass behavior for a particular container with mass coefficients c and k must be analyzed for individual, fixed $\left(\frac{b}{w}\right)$ values for the range of $\left(\frac{B}{w}\right)$ values $1 \leq \left(\frac{B}{w}\right) \leq \left(\frac{b}{w}\right)$.

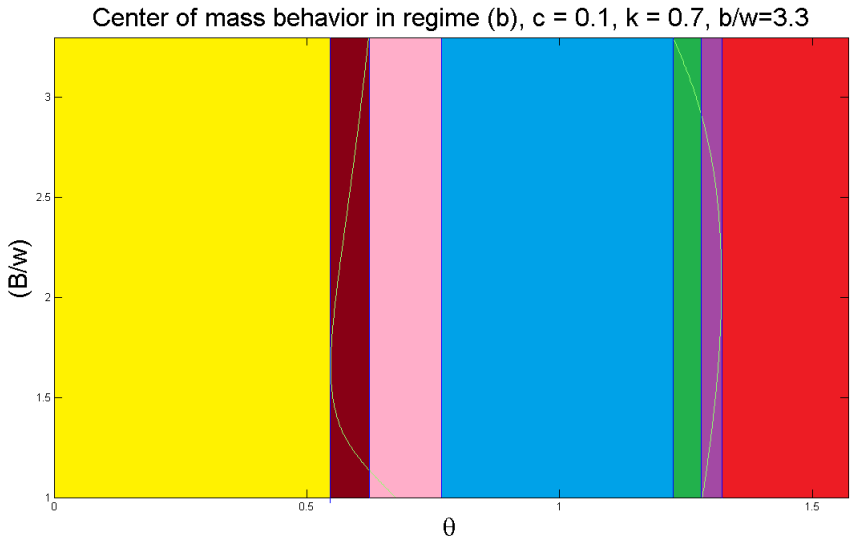

Figure 16: Parameter-space graph for a container with center of mass coefficients $c = 0.1$, $k = 0.7$ and base-to-slot-width ratio $\left(\frac{b}{w}\right) = 3.3$ highlighting its center of mass' behavior in tilted fluid geometry regime (b).

Figure (16) shows one such $\left(\frac{B}{w}\right)$-versus-θ graph for a container with coefficients $c = 0.1$ and $k = 0.7$ for a fixed $\left(\frac{b}{w}\right)$ ratio of 3.3. The red-shaded region indicates θ values for which the center of mass is always past the balancing window in regime (b). The purple-shaded area indicates θ values at which the center of mass reenters the balancing window and subsequently overshoots it in regime (b). The green portion of the graph corresponds to angles for which the center of mass reenters the window and remains there in regime (b). The blue-shaded area is associated with θ values for which the center of mass is always inside of the balancing window in geometric regime (b). The pink-shaded region corresponds to angles for which the center of mass leaves the window in regime (b) and remain short of it. The burgundy-shaded region is associated with values of θ for which the center of mass enters the balancing window in (b), leaves it in (b) and remains short of it. Finally, the yellow shaded region denotes angles for which the center of mass is always short of the balancing window in regime (b).

With parameter-space graphs like Figures (15) and (16), a general outline of the center-of-mass behavior for a particular single-slotted container with base b, slot width w, balancing angle θ and container mass coefficients c and k can be predicted.

2.6.2 Illustrative center of mass trajectories incorporating the container's mass

To illustrate the center of mass behavior described abstractly in Figures (15) and (16), the system's center of mass, $\bar{x}'_{tot}$, will be plotted inside of the container with y values equal to the corresponding untilted fluid height h. This is because as h gets lower, the system's center of mass trajectory doubles back on itself, eventually converging on the container's center of mass, $\left(\bar{X}, \bar{Y}\right)$. As a result, plotting $(\bar{x}'_{tot}, \bar{y}'_{tot})$ makes the trajectory unnecessarily difficult to parse. Fortunately, $\bar{y}'_{tot}$ does not contribute to whether or not the container will balance so its omission does not result in a loss of any information meaningful to this analysis.

In these graphs, the green curve represents $(\bar{x}'_{tot}, h)$. The blue curve corresponds to $(\bar{x}, h)$, showing the fluid's center of mass. The red X shows the location of the container's center of mass. The dashed black lines denote the balance window. Finally, the red lines show the edges of the single-slotted container being analyzed.

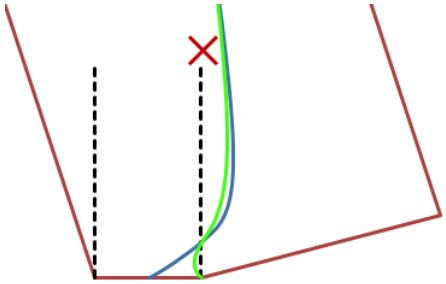

Figure 17: Center of mass trajectory for $\left(\frac{b}{w}\right) = 3.3$, $c = 0.1$, $k = 0.7$ and $\theta = 73.63°$.

Figure (17) shows a container for which its center of mass sits just past the balancing window. As a result, the system's total center of mass overshoots the window in regime (a), then reenters in regime (b) and overshoots the window again in regime (b). The container's geometry and its center of mass' behavior correspond to the pink-shaded region of Figure (15) and the purple-shaded region of Figure (16).

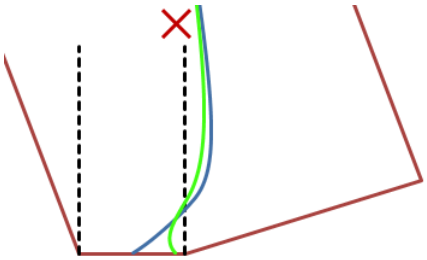

Figure 18: Center of mass trajectory for $\left(\frac{b}{w}\right) = 3.3$, $c = 0.1$, $k = 0.7$ and $\theta = 71.05°$.

Figure (18) shows a container whose center of mass center of mass is just inside the right side of the balancing window. As such, the container-fluid system's center of mass overshoots the window in regime (a), then reenters the balancing window in regime (b) and remains there. The container's geometry and its center of mass' behavior correspond to the pink-shaded region of Figure (15) and the green-shaded region of Figure (16).

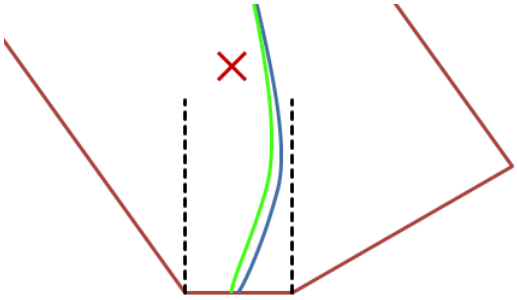

Figure 19: Center of mass trajectory for $\left(\frac{b}{w}\right) = 3.3$, $c = 0.1$, $k = 0.7$ and $\theta = 57.30°$.

Figure (19) illustrates the center of mass trajectory for a container whose center of mass lay firmly inside of the balancing window. The system's center of mass enters the balancing window in regime (a), then never leaves it in either regime. This behavior of indicative of the green-shaded region of Figure (15) and the blue-shaded region of Figure (16).

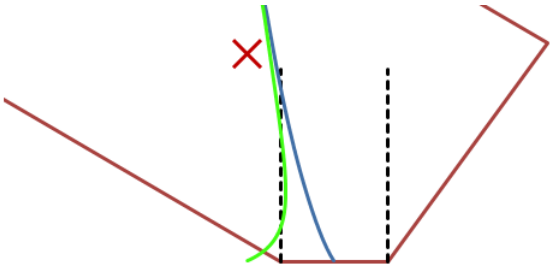

Figure 20: Center of mass trajectory for $\left(\frac{b}{w}\right) = 3.3$, $c = 0.1$, $k = 0.7$ and $\theta = 33.23°$.

Figure (20) shows the total center of mass behavior for a container whose center of mass sits just outside the window of balance. The center of mass of the container-fluid system enters the balancing window in regime (b) and subsequently leaves it to fall short of the window, also in regime (b). The container's geometry and the system's center-of-mass trajectory correspond to the red-shaded area of Figure (15) and the burgundy region of Figure (16).

Worth noting is that the behavior seen in Figure (20), where balance is achieved for a range of h values but otherwise the system's center of mass falls short of the window, is the behavior observed when attempting to balance a real-life twelve-ounce aluminum can on its beveled edge. Thus, the familiar behavior of real-world cans has been recovered by the two-dimensional, single-slotted model.

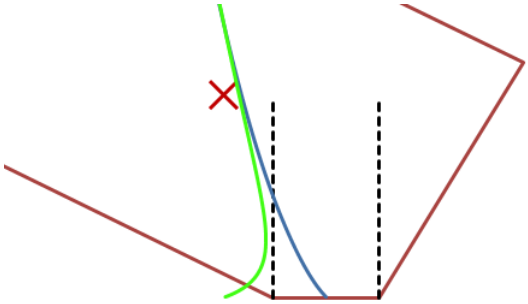

Figure 21: Center of mass trajectory for $\left(\frac{b}{w}\right) = 3.3$, $c = 0.1$, $k = 0.7$ and $\theta = 28.65°$.

Figure (21) shows the center of mass behavior of a container whose own center of mass falls relatively far short of the balancing window. The system's center of mass never reaches the window of balance. This behavior corresponds to the red-shaded region of Figure (15) and the yellow-shaded region of Figure (16).

3 Conclusion

Three two-dimensional models of fluid containers have been examined. The analysis of these containers has fully mapped out the interplay between the models' physical parameters and achieving balance.

For the massless rectangular container, balance can always be achieved. Its balancing angle is determined by by a function, Eq. (7), of the ratio of its base to the untilted fluid height in the container.

Similarly, for the massless single-slotted container which balances at a fixed angle, θ, balance can always be achieved for ranges of untilted fluid heights specific to the geometry of the container. The behavior of the fluid's center of mass is determined by the inequalities of Eqs. (32), (38) and (39). These inequalities are mapped out in the $\left(\frac{b}{w}\right)$-versus-θ parameter-space graph of Figure (11), which illustrates the the behavior of the fluid's center of mass in the container.

Finally, the single-slotted container's own mass was taken into consideration to give a more accurate model of balancing a real-world twelve-ounce aluminum can on its beveled edge. Parameter-space graphs like Figures (15) and (16) can be used to fully map out the fluid-container system's center of mass' behavior for any container. It was also demonstrated that this model can produce the behavior observed when balancing twelve-ounce cans.

Despite using a simplified, two-dimensional model of an aluminum can, the nuances of the behavior observed in the real world have been recreated. An analysis of this model has shown that the depth of the problem is not lost in the simplicity of the model.

Appendix A Crossover h values

From Figure (6), it's clear that any transition between untilted regimes I and II occurs when the fluid is at the top edge of the slot. These crossover heights, then, are

$$h_{I,IIa} = h_{I,IIb} = h_{Ia,IIb} = w\cos\theta. \tag{55}$$

From Figure (6), the transition between tilted regimes (a) and (b) clearly occurs when the level of the tilted fluid is at the corner of the base of the can. The area at this transition is expressed as

$$A_{a,b} = \frac{b^2}{2\tan\theta} - \frac{1}{2}w^2\sin\theta\cos\theta. \tag{56}$$

Setting Eq. (15), the area of fluid in untilted regime I, equal to Eq. (56) and solving for h yields the next crossover height,

$$h_{Ia,b} = \frac{b}{2\tan\theta}. \tag{57}$$

Finally, setting Eq. (16), the area of fluid in untilted regime II, equal to Eq. (56) yields the quadratic

$$\frac{1}{2}\tan\theta h^2 + (b - w\sin\theta)\,h + \frac{1}{2}w^2\sin\theta\cos\theta - \frac{b^2}{2\tan\theta} = 0, \tag{58}$$

with solutions

$$h_{IIa,b} = \frac{-(b - w\sin\theta) \pm \sqrt{2b\,(b - w\sin\theta)}}{\tan\theta}. \tag{59}$$

Because only positive values of h are physical, the negative solution to the quadratic is rejected, yielding the final crossover height,

$$h_{IIa,b} = \frac{-(b - w\sin\theta) + \sqrt{2b\,(b - w\sin\theta)}}{\tan\theta}. \tag{60}$$